



# An experimental and numerical study of the thermal oxidation of chlorobenzene

Brian Higgins<sup>a,\*</sup>, Murray J. Thomson<sup>b</sup>, Donald Lucas<sup>c</sup>,  
Catherine P. Koshland<sup>d</sup>, Robert F. Sawyer<sup>d</sup>

<sup>a</sup> California Polytechnic University, San Luis Obispo, CA, USA

<sup>b</sup> University of Toronto, Canada

<sup>c</sup> Lawrence Berkeley National Laboratory, Berkeley, CA, USA

<sup>d</sup> University of California, Berkeley, CA, USA

## Abstract

A combustion-driven flow reactor was used to examine the formation of chlorinated and non-chlorinated species from the thermal oxidation of chlorobenzene under post-flame conditions. Temperature varied from 725 to 1000 K, while the equivalence ratio was held constant at 0.5. Significant quantities of chlorinated intermediates, vinyl chloride and chlorophenol, were measured. A dominant C–Cl scission destruction pathway seen in pyrolytic studies was not observed. Instead, hydrogen-abstraction reactions prevailed, leading to high concentrations of chlorinated byproducts. The thermal oxidation of benzene was also investigated for comparison.

Chemical kinetic modeling of benzene and chlorobenzene was used to explore reaction pathways. Two chlorobenzene models were developed to test the hypothesis that chlorobenzene oxidation follows a CO-expulsion breakdown pathway similar to that of benzene. For the temperatures and equivalence ratio studied, hydrogen abstraction by hydroxyl radicals dominates the initial destruction of both benzene and chlorobenzene. Chlorinated byproducts (i.e., chlorophenol and vinyl chloride) were formed from chlorobenzene oxidation in similar quantities and at similar temperatures to their respective analogue formed during benzene oxidation (i.e., phenol and ethylene). © 2001 Elsevier Science Ltd. All rights reserved.

## 1. Introduction

Thermal oxidation of chlorinated hydrocarbons in an incinerator is a common waste-disposal method. Under ideal conditions, chlorinated hydrocarbons oxidize to H<sub>2</sub>O, CO<sub>2</sub> and HCl. The HCl can be removed easily with exhaust gas processing. Equilibrium concentrations of parent and intermediate species are negligible (Yang et al., 1987). However, in a poorly operating hazardous waste incinerator, chlorinated hydrocarbons can escape the flame zone and exist in the post-flame region, where chemical-kinetic limitations can lead to the production

of hazardous emissions. Transient or upset conditions, cold-wall impingement, poor atomization of liquid waste, and rogue droplets are examples of poor operating conditions (Oppelt, 1986). Waste-incinerator upset conditions can be replicated in a laboratory environment with a flow reactor. Flow reactor studies are useful because they have measurable boundary conditions, repeatable operation, and can be operated on a scale many times smaller than a waste incinerator. For these reasons, flow reactors are used often to investigate and to predict the reactions that occur in large-scale waste incinerators.

Chlorobenzene decomposition is of interest as the chlorine atom is bonded strongly to the benzene ring (Tsang, 1990) and potentially contributes to dioxin formation (Ritter and Bozzelli, 1990, 1994; Sommeling et al., 1993). A number of studies have examined

\* Corresponding author. Present address: Mech. Eng. Dept., Cal. Poly., San Luis Obispo, CA 93407 USA.

E-mail address: bshiggin@calpoly.edu (B. Higgins).

chlorobenzene reactions, focusing on the removal of the chlorine atom. Tsang (1990), Ritter and Bozzelli (1990), and Manion and Louw (1990) found that chlorine displacement by atomic hydrogen dominates over chlorine abstraction at post-flame temperatures. Ritter and Bozzelli (1990) found that in an  $H_2/O_2$  reaction system,  $O_2$  catalyzed Cl abstraction from chlorobenzene by H atom. Martinez et al. (1995) suggests that  $HO_2$  attack is a major pathway of chlorobenzene destruction in the presence of  $H_2O_2$ . Tsang (1990) stated that chlorination of the aromatic ring is not favored. Senkan (1993) studied premixed, laminar chlorobenzene flames and detected chlorinated intermediates in both fuel-rich and fuel-lean flames. The formation of chlorinated byproducts under post-flame conditions has not been studied in depth.

A detailed understanding of chlorobenzene destruction is strengthened with insight gained from studying benzene reactions and its decomposition products. Most of the chemical-kinetic development, for aromatic compounds, has been under pyrolytic conditions to investigate soot and polycyclic aromatic hydrocarbon (PAH) formation. There are some notable exceptions. Venkat et al. (1982) and Lovell et al. (1988) have studied the oxidation of benzene in an adiabatic flow reactor. A number of chemical-kinetic benzene mechanisms have been published (e.g., Bittker, 1991; Emdee et al., 1992; Zhang and McKinnon, 1995; Marinov et al., 1996; Tan and Frank, 1996). Oxidative benzene reactions are generally understood. However, chemical-kinetic mech-

anisms have not developed completely for every important intermediate species.

This study uses flow reactor experiments and chemical-kinetic modeling to explore the reaction pathways of chlorobenzene at moderate temperatures and fuel-lean conditions. The study focuses on the analogies between benzene and chlorobenzene oxidation. These two compounds are separately injected into a flow reactor; the concentrations of these species and their decomposition products are measured and compared. This experimental data is also used to validate the chemical kinetic models. The modeling provides a more detailed examination of the injected compound's reaction pathways.

## 2. Experimental data

Intermediate species from chlorobenzene oxidation were studied by injecting benzene ( $C_6H_6$ ) or chlorobenzene ( $C_6H_5Cl$ ) into a non-isothermal, combustion-driven flow reactor. This reactor operated with peak temperatures between 700 and 1200 K, an equivalence ratio of 0.5, and residence times near 0.3 ms. Gas composition was measured downstream, along the flow-reactor centerline, using extractive sampling and a Fourier-transform infrared (FTIR) spectrometer.

The flow reactor, schematically illustrated in Fig. 1, was capable of independent control of residence time, equivalence ratio, and peak temperature. Combustion products were delivered to the flow reactor from two

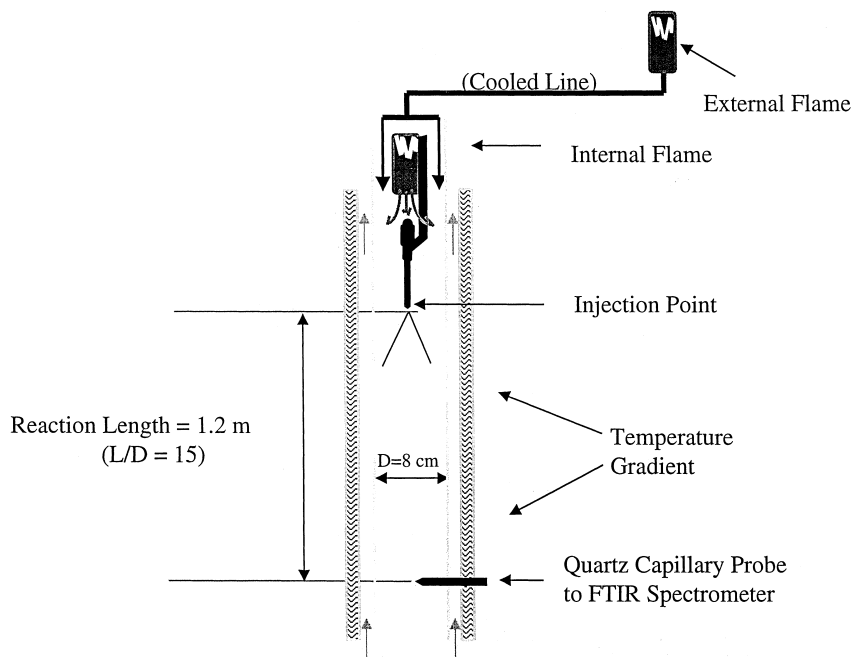


Fig. 1. Schematic representation of the combustion-driven flow reactor. The external flame is cooled and mixed with the internal flame upstream from the point of injection. Products are extracted along the centerline, 1.2 m downstream of the injection point.

sources. Temperature control was achieved by cooling one of the combustion-product sources and mixing it with the non-cooled source. By changing the relative flow through the two combustion sources, the temperature in the flow reactor was varied without altering the equivalence ratio. Each combustion source was operated at an equivalence ratio of 0.92. An equivalence ratio of 0.5 was achieved by mixing secondary air at the point where the combustion sources were mixed. The total flowrate was held constant at 350 slpm. The temperature was held constant with an active-feedback-control system, which varied the relative flowrate of the two combustion sources to maintain a fixed temperature upstream of the injection point. The control system was automated with a computerized control system, thermocouples, and mass-flow controllers. Details of the experimental setup are given by Higgins (1995).

The flow reactor was operated in a non-isothermal mode. Heat transfer to the wall was augmented by a counter flow of air in the annular region between the flow reactor and the water jacket. This enabled efficient data acquisition as the flow reactor quickly achieved steady state. Since the flow reactor was not isothermal, the centerline temperature profile within the reactor was experimentally measured for each condition. These measured temperature profiles are plotted in Fig. 2 for the chlorobenzene injection case; the profiles for benzene are nearly identical. The temperature profiles were used as the thermal boundary condition for chemical-kinetic modeling. Note that they exhibit a characteristic shape. There is an initial increase in temperature, a point of peak temperature, and finally a steady decrease in temperature. The initial increase in the centerline temperature occurs during the mixing process of the injected species with the main flow of combustion products; details are discussed by Higgins (1995). The steady decrease in temperature near the end of the flow is due to heat transfer to the wall. Temperatures drop from 50 to

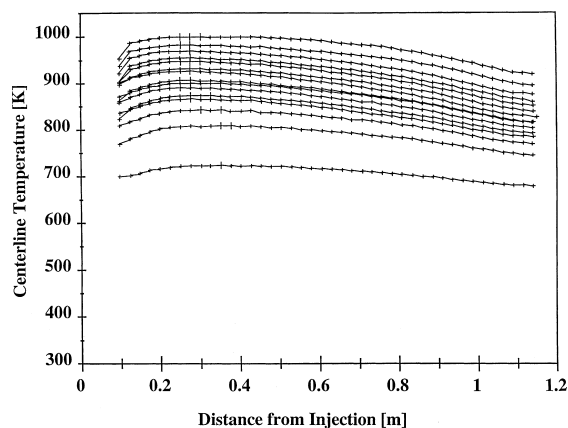


Fig. 2. Measured centerline temperature for chlorobenzene injection.

80 K at a rate of approximately 300 K/s for the flowrates used in this study. The combined effect of mixing and heat transfer to the wall produces a peak temperature in the flow that is located downstream of the point of injection. This measured peak temperature is the temperature used to plot the data in later figures.

By injecting the benzene and chlorobenzene along the centerline of the reactor, wall effects were reduced, but this created a region of unmixedness that was not included in the numerical model. This presents a limitation in the utility of the model, and became the primary reason for injecting both benzene and chlorobenzene. The published mechanisms for benzene oxidation are assumed to be, and are shown to be, sufficient to document the general trends observed in the benzene experiments. By modeling both benzene and chlorobenzene, only the relative differences and similarities between the two are important, and findings are not diluted by the limitations of the model. Secondly, the important reactions are highly temperature dependent and although the benzene and chlorobenzene are injected in an unmixed fashion, by the time the maximum temperature is reached, they are well mixed.

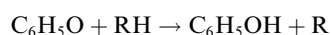
Gas species compositions were measured using extractive sampling and a FTIR spectrometer. Species were extracted from the centerline of the flow reactor through a quartz capillary probe, and were carried from the flow reactor to the FTIR, through heated Teflon tubing. The byproducts were measured with a Biorad FTS-40 FTIR spectrometer coupled to an infrared analysis, long path cell (0.6 m base path length, 14.4 m total path length). A needle valve at the exit of the optical cell was used to maintain a pressure of 71 Torr in the cell. With a vacuum pump downstream of this valve and the capillary probe upstream, the flow through the cell was continuous. Stable measurements were possible after about 20 min of sampling. The FTIR was calibrated by injecting liquid or gaseous species into an evacuated cell and adding nitrogen to 71 Torr. All calibrated species are expected to have an error of  $\pm 20\%$  (Hall et al., 1991) except for hydrogen chloride. Hydrogen chloride was difficult to calibrate due to absorption to the optical cell walls. Errors in the hydrogen chloride calibrations are assumed to be less than  $\pm 50\%$  (Higgins, 1995). Although absolute concentrations exhibit large errors, the concentration of any one species has much less relative error.

A carbon balance for benzene – or chlorobenzene – cannot be given. The amount of  $\text{CO}_2$  in the combustion products was approximately 8% of the total flow, and benzene – injected at 563 ppm – only accounts for 4% of the total carbon in the system. Since an FTIR is not able to measure  $\text{CO}_2$  with an accuracy of 4%, a carbon balance is not included.

The walls of the combustor were constructed with stainless steel. Several experiments were run with a quartz liner to address the possibility of catalytic reactions

of chlorinated hydrocarbons on the stainless-steel surfaces. All stainless steel in the flow path was eliminated from the flow reactor and the extractive sampling lines. With the quartz liner, there were no observable differences in the gas species concentrations. Wall effects were not observed since the turbulent mixing time within the flow reactor was of the same order of time as the convective flow time. Thus, the chlorinated hydrocarbons did not have sufficient time to flow from the centerline of the flow reactor to the wall and back to the centerline where the gasses were sampled (Higgins, 1995).

Species were sampled through a quartz capillary probe at low pressure. Reactions in the probe can convert radical species into stable species that are not formed directly in the flow reactor. Lovell et al. (1988) and Brezinsky et al. (1990) propose that conversion of phenoxy to phenol is common in probes. This reaction



is aided by the large quantities of hydrogen from combustion products. Likewise, this suggests that chlorinated phenoxy radicals will undergo the same hydration process. Effectively, measured phenol represents both phenol and phenoxy sampled from the flow reactor. Therefore, when a phenoxy radical was predicted by the model, it was assumed to hydrate in the probe. In the figures, predicted phenoxy-radical concentrations were added to the phenol concentrations. Likewise, predicted chlorophenol and chlorophenoxy radical concentrations were added together.

The intent of using a non-isothermal, combustion-driven flow reactor was to simulate conditions expected in the post-flame region of a hazardous waste incinerator during a failure mode. Heat loss, oxygen concentration, residence time, POHC concentrations, and turbulence levels were designed to model those found in a large-scale incinerator. This lab-scale flow reactor was also designed to have controlled and measurable boundary conditions to facilitate modeling. The balance of these features allowed the measurement and prediction of a real-life situation within the bounds and expectations of a laboratory measurement system. Discrepancies in the plug-flow-reactor assumption used for modeling are made up through the direct comparison of data from two species (e.g., the more studied benzene versus the less studied chlorobenzene).

### 3. Numerical model and mechanisms

Numerical modeling of the chemical processes in the flow reactor was performed using the CHEMKIN package (Kee et al., 1990) with a plug-flow-reactor (PFR) assumption (Chen, 1992). Measured centerline temperatures were used to constrain the temperature in the PFR model. The inlet boundary condition for the plug flow reactor model assumed that the combustion

product flow was in chemical-kinetic thermodynamic equilibrium at the temperature measured just upstream of the point of injection.

Benzene was modeled using five published chemical-kinetic mechanisms. The mechanism of Tan and Frank (1996) gave no significant benzene oxidation in the temperature range studied, which was not unexpected since their mechanism was developed for a rich, near-sooting flame. The mechanism of Bittker (1991) had results that were significantly dissimilar to the experimental results. Three are analyzed further in this paper: Emdee et al. (1992), Zhang and McKinnon (1995), and Marinov et al. (1996). Both the Zhang and McKinnon (1995) and Marinov et al. (1996) mechanisms incorporated portions of the Emdee et al. (1992) mechanism.

The benzene mechanism of Zhang and McKinnon (1995) was developed at low pressures and required modification. Specifically, the mechanism reaction rates were modified for atmospheric pressure using the original references and the QRRK method (Dean, 1985). The CHEMACT computer code (Dean et al., 1991) was used for QRRK calculations along with the parameters given by Zhang and McKinnon (1995). The molecular thermodynamic data of Zhang and McKinnon (1995) were also used.

Chlorobenzene data was modeled using two aggregate chlorobenzene-oxidation mechanisms. One was based on the benzene mechanism of Zhang and McKinnon (1995) and the other on Marinov et al. (1996). No rate constants were adjusted to fit the experimental data. The aggregate mechanism contained reactions from six sources: (1) parent benzene sub-mechanism (Zhang and McKinnon, 1995; or Marinov et al., 1996), (2) CO/H<sub>2</sub>O/HCl reaction sub-system of Roesler et al. (1992), (3) Cl/hydrocarbon reactions (Senkan, 1993), (4) chlorinated C<sub>1</sub> and C<sub>2</sub> sub-mechanism of Qun and Senkan (1994), (5) individual chlorobenzene and chlorophenol reactions from various literature sources (e.g., Mallard et al., 1998), and (6) reactions developed in the discussion section of this paper. More details are provided in later sections. Whenever possible, literature molecular thermodynamic data was used. Otherwise, the computer program THERM (Ritter and Bozzelli, 1991) was used to calculate thermodynamic parameters of radicals and molecular species based on the methods of Benson group additivity, and properties of radicals based on bond dissociation.

Using the above approach, two chlorobenzene mechanisms have been produced. Each mechanism contains the original reactions of the parent benzene mechanism. The chlorobenzene mechanisms developed for this paper are used for analysis only and have not been tested against data from other temperature and mixture regimes. The reaction rates used in this study are included in Tables 1–3. Table 1 contains 37 reactions added to both the Zhang and McKinnon mechanism and the Marinov et al. mechanism. In Table 2, are the 35 reactions

Table 1

Reactions present in both chlorobenzene mechanisms (in cal-K-gmole-cm-s units)

Reaction	A	n	Ea	Source
CO & HCl submechanism				Roesler et al., 1995
Chlorinated C <sub>1</sub> and C <sub>2</sub> submechanism				Qun and Senkan, 1994
Reactions of C <sub>1</sub> through C <sub>6</sub> hydrocarbons with Cl and ClO				Qun and Senkan, 1994
C <sub>6</sub> H <sub>5</sub> Cl+O = C <sub>6</sub> H <sub>5</sub> +ClO	1.00E+08	2	37600	Qun and Senkan, 1994
C <sub>6</sub> H <sub>5</sub> Cl = C <sub>6</sub> H <sub>5</sub> +Cl	3.00E+15	0	95499	Ritter and Bozzelli, 1990
C <sub>6</sub> H <sub>5</sub> Cl = <i>o</i> -C <sub>6</sub> H <sub>4</sub> Cl+H	5.20E+15	0	110000	Martinez et al., 1995 <sup>a</sup>
C <sub>6</sub> H <sub>5</sub> Cl = <i>m</i> -C <sub>6</sub> H <sub>4</sub> Cl+H	5.20E+15	0	110000	Martinez et al., 1995 <sup>a</sup>
C <sub>6</sub> H <sub>5</sub> Cl = <i>p</i> -C <sub>6</sub> H <sub>4</sub> Cl+H	2.60E+15	0	110000	Martinez et al., 1995 <sup>a</sup>
C <sub>6</sub> H <sub>5</sub> Cl+H = C <sub>6</sub> H <sub>6</sub> +Cl	1.50E+13	0	7500	Ritter and Bozzelli, 1990
C <sub>6</sub> H <sub>5</sub> Cl+H = C <sub>6</sub> H <sub>5</sub> +HCl	2.00E+13	0	6450	Manion et al., 1988
C <sub>6</sub> H <sub>5</sub> Cl+H = <i>o</i> -C <sub>6</sub> H <sub>4</sub> Cl+H <sub>2</sub>	4.00E+12	0	12000	Louw et al., 1973 <sup>a</sup>
C <sub>6</sub> H <sub>5</sub> Cl+H = <i>m</i> -C <sub>6</sub> H <sub>4</sub> Cl+H <sub>2</sub>	4.00E+12	0	12000	Louw et al., 1973 <sup>a</sup>
C <sub>6</sub> H <sub>5</sub> Cl+H = <i>p</i> -C <sub>6</sub> H <sub>4</sub> Cl+H <sub>2</sub>	2.00E+12	0	12000	Louw et al., 1973 <sup>a</sup>
C <sub>6</sub> H <sub>5</sub> Cl+Cl = <i>o</i> -C <sub>6</sub> H <sub>4</sub> Cl+HCl	1.20E+12	0	12800	Martinez et al., 1995 <sup>a</sup>
C <sub>6</sub> H <sub>5</sub> Cl+Cl = <i>m</i> -C <sub>6</sub> H <sub>4</sub> Cl+HCl	1.20E+12	0	12800	Martinez et al., 1995 <sup>a</sup>
C <sub>6</sub> H <sub>5</sub> Cl+Cl = <i>p</i> -C <sub>6</sub> H <sub>4</sub> Cl+HCl	6.00E+11	0	12800	Martinez et al., 1995 <sup>a</sup>
C <sub>6</sub> H <sub>5</sub> Cl+OH = C <sub>6</sub> H <sub>5</sub> OH+Cl	5.00E+12	0	14000	Martinez et al., 1995
C <sub>6</sub> H <sub>5</sub> Cl+O = C <sub>6</sub> H <sub>5</sub> O+Cl	5.00E+12	0	13000	Martinez et al., 1995
C <sub>6</sub> H <sub>5</sub> Cl+O = <i>o</i> -C <sub>6</sub> H <sub>4</sub> ClO+H	8.40E+12	0	4763	Frerichs et al., 1989 <sup>a</sup>
C <sub>6</sub> H <sub>5</sub> Cl+O = <i>m</i> -C <sub>6</sub> H <sub>4</sub> ClO+H	8.40E+12	0	4763	Frerichs et al., 1989 <sup>a</sup>
C <sub>6</sub> H <sub>5</sub> Cl+O = <i>p</i> -C <sub>6</sub> H <sub>4</sub> ClO+H	4.20E+12	0	4763	Frerichs et al., 1989 <sup>a</sup>
<i>o</i> -C <sub>6</sub> H <sub>4</sub> ClOH+H = C <sub>6</sub> H <sub>5</sub> OH+Cl	4.35E+13	0	8243	Manion and Louw, 1990
<i>m</i> -C <sub>6</sub> H <sub>4</sub> ClOH+H = C <sub>6</sub> H <sub>5</sub> OH+Cl	2.69E+13	0	8243	Manion and Louw, 1990
<i>p</i> -C <sub>6</sub> H <sub>4</sub> ClOH+H = C <sub>6</sub> H <sub>5</sub> OH+Cl	4.05E+13	0	8243	Manion and Louw, 1990
<i>o</i> -C <sub>6</sub> H <sub>4</sub> ClOH+H = C <sub>6</sub> H <sub>5</sub> Cl+OH	3.11E+13	0	8243	Manion and Louw, 1990
<i>m</i> -C <sub>6</sub> H <sub>4</sub> ClOH+H = C <sub>6</sub> H <sub>5</sub> Cl+OH	2.14E+13	0	8243	Manion and Louw, 1990
<i>p</i> -C <sub>6</sub> H <sub>4</sub> ClOH+H = C <sub>6</sub> H <sub>5</sub> Cl+OH	2.51E+13	0	8243	Manion and Louw, 1990
<i>o</i> -C <sub>6</sub> H <sub>4</sub> ClO+H = C <sub>6</sub> H <sub>5</sub> O+Cl	1.50E+13	0	7500	Estimate
<i>m</i> -C <sub>6</sub> H <sub>4</sub> ClO+H = C <sub>6</sub> H <sub>5</sub> O+Cl	1.50E+13	0	7500	Estimate
<i>p</i> -C <sub>6</sub> H <sub>4</sub> ClO+H = C <sub>6</sub> H <sub>5</sub> O+Cl	1.50E+13	0	7500	Estimate
<i>o</i> -C <sub>6</sub> H <sub>4</sub> Cl+H = C <sub>6</sub> H <sub>5</sub> +Cl	1.50E+13	0	7500	Estimate
<i>m</i> -C <sub>6</sub> H <sub>4</sub> Cl+H = C <sub>6</sub> H <sub>5</sub> +Cl	1.50E+13	0	7500	Estimate
<i>p</i> -C <sub>6</sub> H <sub>4</sub> Cl+H = C <sub>6</sub> H <sub>5</sub> +Cl	1.50E+13	0	7500	Estimate
ClC <sub>5</sub> H <sub>4</sub> +H = C-C <sub>5</sub> H <sub>5</sub> +Cl	1.50E+13	0	7500	Estimate
C <sub>5</sub> H <sub>4</sub> ClO+H = C-C <sub>5</sub> H <sub>5</sub> O+Cl	1.50E+13	0	7500	Estimate
C <sub>4</sub> H <sub>4</sub> Cl = H <sub>2</sub> CCCCH <sub>2</sub> +Cl	1.00E+13	0	40300	Qun and Senkan, 1994
C <sub>4</sub> H <sub>4</sub> Cl+OH = H <sub>2</sub> CCCCH <sub>2</sub> +HOCl	1.00E+07	2	0	Qun and Senkan, 1994
C <sub>4</sub> H <sub>4</sub> Cl+O = H <sub>2</sub> CCCCH <sub>2</sub> +ClO	1.00E+07	2	0	Qun and Senkan, 1994
C <sub>4</sub> H <sub>4</sub> Cl+H = H <sub>2</sub> CCCCH <sub>2</sub> +HCl	1.00E+07	2	0	Qun and Senkan, 1994
C <sub>4</sub> H <sub>4</sub> Cl+Cl = H <sub>2</sub> CCCCH <sub>2</sub> +Cl <sub>2</sub>	1.00E+07	2	0	Qun and Senkan, 1994

<sup>a</sup> isomerization added.

added only to the Zhang and Mckinnon mechanism and in Table 3 are the 22 reactions added only to the Marinov et al. mechanism. More work is needed to verify the reactions with estimated rates. Great care should be taken when using these rates, particularly for conditions not representative of the conditions found in this study.

#### 4. Results and discussion

Benzene or chlorobenzene was injected to give initial concentrations of 563 or 719 ppm, respectively. In

Fig. 3, normalized destruction profiles for benzene and chlorobenzene are plotted versus the peak flow-reactor temperature; the profiles are quite similar. The first indication that both benzene and chlorobenzene are reacting is seen between 800 and 850 K. Benzene exhibits slightly higher reactivity, reaching 50% oxidation at 950 K compared to 960 K for chlorobenzene. By 993 K, more than 97% of the injected benzene was destroyed, converted to products or intermediates. Likewise, by 1000 K, over 96% of the chlorobenzene was destroyed.

Table 2

Additional reactions present in the mechanism based on the benzene mechanism of Zhang and McKinnon, 1995 (in cal-K-gmole-cm-s units)

Reaction	A	<i>n</i>	E <sub>a</sub>	Source
Benzene submechanism				
$C_6H_5Cl+OH = o-C_6H_4Cl+H_2O$	1.68E+12	0	4491	Zhang and McKinnon, 1995 Mulder and Louw, 1987 and Zhang and McKinnon, 1995 <sup>a</sup>
$C_6H_5Cl+OH = m-C_6H_4Cl+H_2O$	1.68E+12	0	4491	Mulder and Louw, 1987 and Zhang and McKinnon, 1995 <sup>a</sup>
$C_6H_5Cl+OH = p-C_6H_4Cl+H_2O$	8.42E+11	0	4491	Mulder and Louw, 1987 and Zhang and McKinnon, 1995 <sup>a</sup>
$o-C_6H_4ClOH+OH = o-C_6H_4ClO+H_2O$	2.95E+06	2	-1312	Estimate
$m-C_6H_4ClOH+OH = m-C_6H_4ClO+H_2O$	2.95E+06	2	-1312	Estimate
$p-C_6H_4ClOH+OH = p-C_6H_4ClO+H_2O$	2.95E+06	2	-1312	Estimate
$o-C_6H_4ClO+H = o-C_6H_4ClOH$	7.24E+47	-9.7	20190	Estimate
$m-C_6H_4ClO+H = m-C_6H_4ClOH$	7.24E+47	-9.7	20190	Estimate
$p-C_6H_4ClO+H = p-C_6H_4ClOH$	7.24E+47	-9.7	20190	Estimate
$o-C_6H_4ClO = ClC_5H_4+CO$	7.41E+11	0	43900	Estimate
$m-C_6H_4ClO = ClC_5H_4+CO$	7.41E+11	0	43900	Estimate
$p-C_6H_4ClO = ClC_5H_4+CO$	7.41E+11	0	43900	Estimate
$o-C_6H_4Cl+O_2 = o-C_6H_4ClO+O$	2.09E+12	0	7470	Estimate
$m-C_6H_4Cl+O_2 = m-C_6H_4ClO+O$	2.09E+12	0	7470	Estimate
$p-C_6H_4Cl+O_2 = p-C_6H_4ClO+O$	2.09E+12	0	7470	Estimate
$o-C_6H_4Cl+O_2 = 2CO+C_2H_2+CHClCH$	3.00E+13	0	15002	Estimate
$m-C_6H_4Cl+O_2 = 2CO+C_2H_2+CHClCH$	3.00E+13	0	15002	Estimate
$p-C_6H_4Cl+O_2 = 2CO+C_2H_2+CHClCH$	3.00E+13	0	15002	Estimate
$o-C_6H_4Cl+O_2 = 2CO+C_2H_2+CH_2CCl$	1.50E+13	0	15002	Estimate
$m-C_6H_4Cl+O_2 = 2CO+C_2H_2+CH_2CCl$	1.50E+13	0	15002	Estimate
$p-C_6H_4Cl+O_2 = 2CO+C_2H_2+CH_2CCl$	1.50E+13	0	15002	Estimate
$o-C_6H_4Cl+O_2 = 2CO+C_2HCl+C_2H_3$	3.00E+13	0	15002	Estimate
$m-C_6H_4Cl+O_2 = 2CO+C_2HCl+C_2H_3$	3.00E+13	0	15002	Estimate
$p-C_6H_4Cl+O_2 = 2CO+C_2HCl+C_2H_3$	3.00E+13	0	15002	Estimate
$ClC_5H_4+HO_2 = C_5H_4ClO+OH$	3.00E+13	0	0	Estimate
$C_5H_4ClO = C_4H_4Cl+CO$	2.51E+11	0	43900	Estimate
$C_4H_4Cl+O_2 = C_4H_3Cl+HO_2$	1.20E+11	0	0	Estimate
$C_4H_3Cl+OH = C_4H_2Cl+H_2O$	7.50E+06	2	5000	Estimate
$C_4H_3Cl+OH = H_2CCCCH+HOCl$	1.00E+06	2.00	44700	Qun and Senkan, 1994
$C_4H_3Cl+O = H_2CCCCH+ClO$	1.00E+07	2.00	36400	Qun and Senkan, 1994
$C_4H_3Cl+M = H_2CCCCH+Cl+M$	1.00E+16	0.00	100800	Qun and Senkan, 1994
$C_4H_3Cl+Cl = H_2CCCCH+Cl_2$	1.00E+07	2.00	42800	Qun and Senkan, 1994
$CH_2CCl+C_2H = C_4H_3Cl$	3.89E+17	1.75	2291	Qun and Senkan, 1994
$C_4H_2Cl+O_2 = CHClCO+HCCO$	0.66E+12	0	0	Estimate
$C_4H_2Cl+O_2 = CH_2CO+C_2ClO$	0.33E+12	0	0	Estimate

<sup>a</sup> isomerization added.

## 5. Benzene oxidation results

The first phase of this study was to evaluate existing benzene chemical-kinetic mechanisms against the experimental results. The experiments span a range of temperatures and species concentrations different from the data originally used to validate the mechanisms. Benzene ( $C_6H_6$ ) oxidation was observed between 850 and 1000 K. The results for  $C_6H_6$  oxidation are plotted in Figs. 4–7. Measured byproducts include phenol ( $C_6H_5OH$ ), formaldehyde ( $CH_2O$ ), ethylene ( $C_2H_4$ ), acetylene ( $C_2H_2$ ) and carbon monoxide (CO). The ultimate products of  $C_6H_6$  oxidation (i.e.,  $CO_2$  and  $H_2O$ ) were observed but not quantified due to the large

quantities of  $CO_2$  and  $H_2O$  in the background combustion-products flow.

In Fig. 4, measured and predicted concentrations of  $C_6H_6$  are plotted versus peak temperature. All the three mechanisms predict that the start of  $C_6H_6$  oxidation occurs above 900 K. Experimental data shows signs of benzene oxidation at temperatures approximately 50 K lower. Complete destruction of the parent species was predicted equally by all the three mechanisms. The mechanism of Marinov et al. (1996) appears to fit the data best.

Data for phenol ( $C_6H_5OH$ ), the only detected aromatic byproduct, are plotted in Fig. 5. The numerical results include both phenoxy ( $C_6H_5O$ ) and  $C_6H_5OH$  as described earlier.  $C_6H_5OH$  was only observed at tem-

Table 3

Additional reactions present in the mechanism based on the benzene mechanism of Marinov et al., 1996 (in cal-K-gmole-cm-s units)

Reaction	A	n	Ea	Source
Benzene submechanism				
$C_6H_5Cl+OH = o-C_6H_4Cl+H_2O$	1.90E+07	1.42	1454	Marinov et al., 1996 Mulder and Louw, 1987 and Marinov et al., 1996 <sup>a</sup>
$C_6H_5Cl+OH = m-C_6H_4Cl+H_2O$	1.90E+07	1.42	1454	Mulder and Louw, 1987 and Marinov et al., 1996 <sup>a</sup>
$C_6H_5Cl+OH = p-C_6H_4Cl+H_2O$	9.00E+06	1.42	1454	Mulder and Louw, 1987 <sup>a</sup>
$o-C_6H_4ClOH+OH = o-C_6H_4ClO+H_2O$	2.95E+06	2	-1310	estimate
$m-C_6H_4ClOH+OH = m-C_6H_4ClO+H_2O$	2.95E+06	2	-1310	Estimate
$p-C_6H_4ClOH+OH = p-C_6H_4ClO+H_2O$	2.95E+06	2	-1310	Estimate
$o-C_6H_4ClO+H = o-C_6H_4ClOH$	1.00E+14	0	0	Estimate
$C_6H_4ClOm+H = m-C_6H_4ClOH$	1.00E+14	0	0	Estimate
$p-C_6H_4ClO+H = p-C_6H_4ClOH$	1.00E+14	0	0	Estimate
$o-C_6H_4ClO = ClC_5H_4+CO$	7.40E+11	0	43850	Estimate
$m-C_6H_4ClO = ClC_5H_4+CO$	7.40E+11	0	43850	Estimate
$p-C_6H_4ClO = ClC_5H_4+CO$	7.40E+11	0	43850	Estimate
$o-C_6H_4Cl+O_2 = o-C_6H_4ClO+O$	2.60E+13	0	6120	Estimate
$m-C_6H_4Cl+O_2 = m-C_6H_4ClO+O$	2.60E+13	0	6120	Estimate
$p-C_6H_4Cl+O_2 = p-C_6H_4ClO+O$	2.60E+13	0	6120	Estimate
$ClC_5H_4+HO_2 = C_5H_4ClO+OH$	3.00E+13	0	0	Estimate
$C_5H_4ClO = C_4H_4Cl+CO$	2.51E+11	0	43900	Estimate
$C_4H_4Cl+O_2 = C_3H_2ClO+CH_2O$	6.00E+11	0	0	Estimate
$C_4H_4Cl+O_2 = CHCHCHO+CHClO$	4.00E+11	0	0	Estimate
$C_3H_2ClO+O_2 = COCl+CHOCHO$	3.00E+12	0	0	Estimate
$C_3H_2ClO = C_2H_2+COCl$	3.30E+13	0	33000	Estimate
$C_3H_2ClO = C_2HCl+HCO$	6.60E+13	0	33000	Estimate

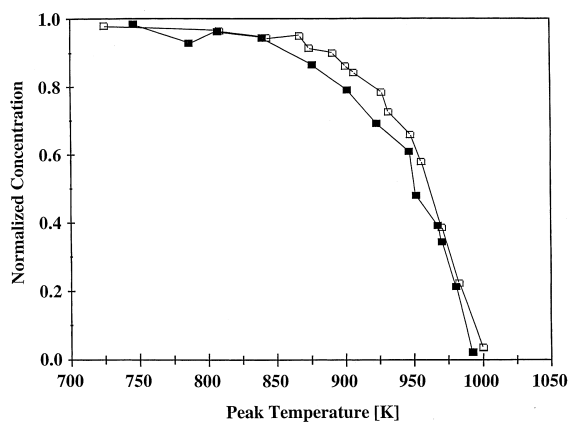
<sup>a</sup> isomerization added.

Fig. 3. Normalized  $C_6H_6$  (filled squares) and  $C_6H_5Cl$  (open squares) outlet concentration for increasing peak temperature. Data normalized to inlet concentrations predicted from flow-rate measurements.

peratures where partial  $C_6H_6$  oxidation is observed. Above 1000 K, where  $C_6H_6$  was fully oxidized,  $C_6H_5OH$  was not observed.  $C_6H_5OH$  peaked near 960 K at a concentration of 201 ppm, or a 71% yield of the reacted  $C_6H_6$ . Below 950 K, the conversion rate of reacted benzene to phenol is between 90% and 100%. The Emdee et al. (1992) mechanism predicted peak  $C_6H_5OH$  concentration

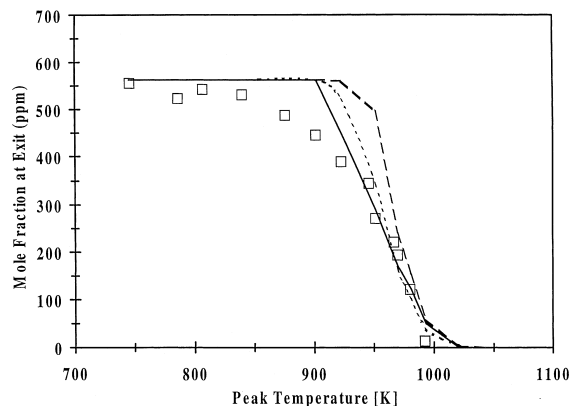


Fig. 4. Outlet concentration of  $C_6H_6$  (squares) for the injection of  $C_6H_6$ . Modeled using the mechanisms of Emdee et al. (dotted line), Zhang and McKinnon (dashed line), and Marinov et al. (solid line).

within a factor of two and adequately described production trends. The Zhang and McKinnon (1995) mechanism also described the formation trends of  $C_6H_5OH$  and the Marinov et al. (1996) mechanism predicted a lower temperature for peak concentration of  $C_6H_5OH$ .

The trends for  $CH_2O$ , Fig. 6, followed that of  $C_6H_5OH$ . Peak concentration occurred at the same temperature (960 K) and at a slightly lower concentra-

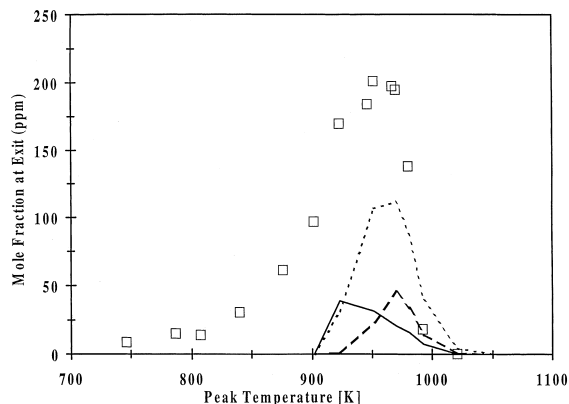


Fig. 5. Outlet concentration of  $C_6H_5OH$  (squares) for the injection of  $C_6H_6$ . Modeled data plotted as the sum of  $C_6H_5OH$  and  $C_6H_5O$ , using the mechanisms of Emdee et al. (dotted line), Zhang and McKinnon (dashed line), and Marinov et al. (solid line).

tion (173 ppm). The mechanism of Emdee et al. (1992) did not include  $CH_2O$ . The  $CH_2O$  data were underpredicted by the other two mechanisms, although both preserved qualitative trends.

In Fig. 7, data for  $C_2H_4$  and  $C_2H_2$  are plotted. Peak concentrations and concentration profiles for both  $C_2H_4$  and  $C_2H_2$  occurred at higher temperatures than was seen for  $C_6H_5OH$  and  $CH_2O$ . At 980 K, concentrations peaked at 33 and 15 ppm, respectively. The profiles peak at higher temperatures relative to  $C_6H_5OH$ , and the species occur later in the destruction pathway than  $C_6H_6$  and  $C_6H_5OH$  (discussed in the next section). The Marinov et al. (1996) mechanism did the best job of modeling  $C_2H_2$  concentrations, but none of the mechanisms predicted significant levels of  $C_2H_4$ .

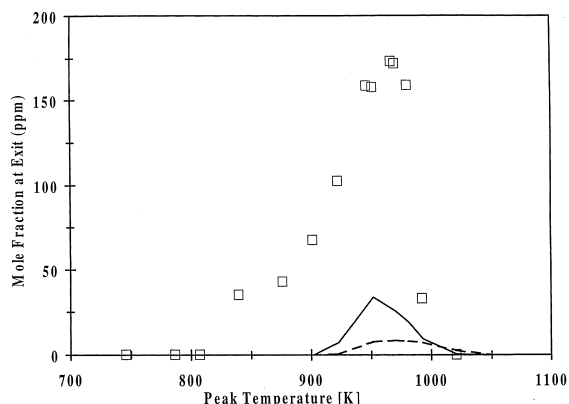


Fig. 6. Outlet concentration of  $CH_2O$  (squares) for the injection of  $C_6H_6$ . Modeled using the mechanisms of Emdee et al. (dotted line), Zhang and McKinnon (dashed line), and Marinov et al. (solid line).

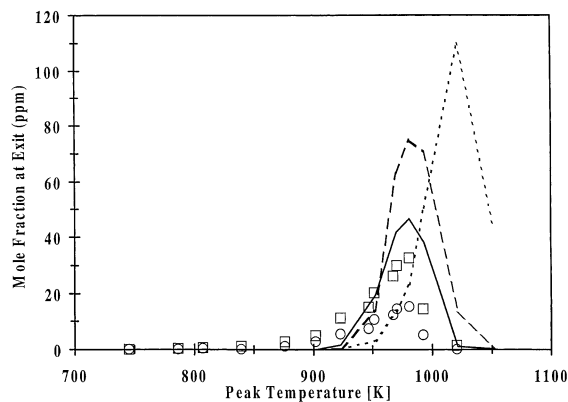


Fig. 7. Outlet concentration of  $C_2H_2$  (squares) and  $C_2H_4$  (circles) for the injection of  $C_6H_6$ . Only  $C_2H_2$  was modeled, using the mechanisms of Emdee et al. (dotted line), Zhang and McKinnon (dashed line), and Marinov et al. (solid line). None of the mechanisms predicted significant  $C_2H_4$ .

All the three benzene-oxidation mechanisms predicted byproducts that were not measured. The Marinov et al. (1996) mechanism predicted significant concentrations of 2,4-cyclohexadienone ( $C_6H_6O$ ), benzoquinone ( $OC_6H_4O$ ), and 2,4-cyclopentadiene-1-one ( $C_5H_4O$ ).  $OC_6H_4O$  peaked at 66 ppm at 993 K.  $C_6H_6O$  and  $C_5H_4O$  continuously increased with temperature, reaching 81 and 160 ppm at the highest temperature condition (1051 K). The Zhang and McKinnon (1995) mechanism predicted 2,4-cyclopentadiene-1-one ( $C_5H_4O$ ) formation. The  $C_5H_4O$  increased with temperature, forming 64 ppm at the highest temperature condition (1051 K). The  $C_4H_4$  radical was predicted to peak at 76 ppm at 1021 K. The Emdee et al. (1992) mechanism also predicts high levels of  $C_4H_4$  and  $C_5H_4O$ .

For near stoichiometric conditions, Emdee et al. (1992) present experimental data including both  $C_4$  and  $C_5$  species as byproducts for benzene oxidation at an equivalence ratio of 0.9. For our conditions, the Emdee et al. mechanism predicted  $C_4$  and  $C_5$  byproduct species. While many of the predicted  $C_4$  and  $C_5$  species are detectable with an FTIR, concentrations above 1 ppm were not detected in our experiments. This discrepancy is probably due to the flow of combustion products in which the benzene is injected. That is, in our experiments benzene is injected at low concentrations into the flow of fuel-lean combustion products. High concentrations of  $H_2O$  and  $CO_2$  alter the chemistry by providing active reacting partners and a source of radical species. Destruction reactions of  $C_4$  and  $C_5$  species in a flow of combustion products are not well characterized in the literature for these temperatures ( $\sim 700$  to 1000 K).

With the exception of lower temperatures, the destruction of  $C_6H_6$  was well predicted by all the three mechanisms. This confirms that much of the  $C_6$  chemistry is valid for our experimental conditions. At low temper-

atures (e.g., 800–900 K), a lack of benzene oxidation and phenol production suggests that some minor changes in the  $C_6$  chemistry is needed. The prediction of minor species requires more work. Discrepancies in  $CH_2O$ ,  $C_2H_2$ , and  $C_2H_4$  concentrations point to incomplete chemistry describing the cascade from  $C_6$  to  $C_2$  species.

## 6. Benzene oxidation destruction pathway (993 K)

The three mechanisms examined were developed sequentially, each expanding on the premise that aromatic-ring oxidation occurs through a CO-expulsion breakdown pathway, reducing the number of carbons in the ring (i.e.,  $C_6 \rightarrow C_5 \rightarrow C_4$ ) until it is no longer stable and a linear species is formed. In general, each carbon-removal step includes an oxygen-addition step and a CO-expulsion step. The CO-expulsion step from a  $C_5$  species breaks the ring, forming either a linear  $C_4$  species or two  $C_2$  molecules.

The general description of  $C_6H_6$  oxidation can be expanded upon and visualized with a reaction pathway. In Figs. 8 and 9, the reaction pathways for the oxidation of  $C_6H_6$  at 993 K are shown using the Zhang and McKinnon (1995) mechanism (Fig. 8) and the Marinov et al. (1996) mechanism (Fig. 9). In these figures, each reaction path is indicated with arrows whose thickness is proportional to the flux through that pathway. A temperature of 993 K was chosen because that was the lowest temperature at which nearly all of the benzene reacted.

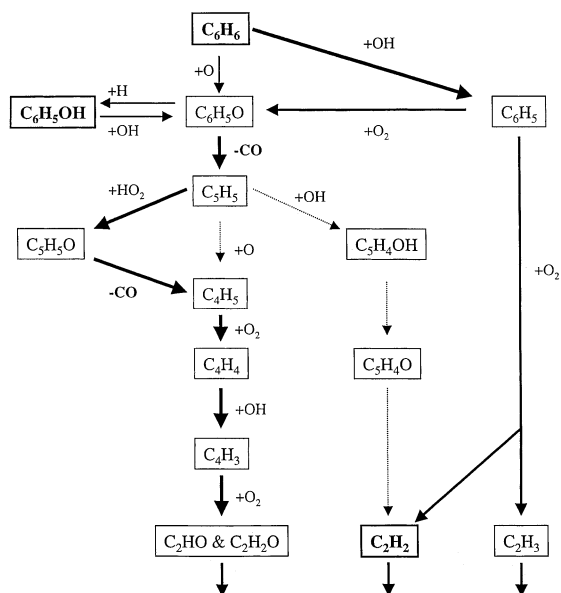


Fig. 8. Destruction-pathway diagram of  $C_6H_6$  at 993 K, using the mechanism of Zhang and McKinnon. Relative flux through pathways are proportional to the arrow width. Species in bold were experimentally measured.

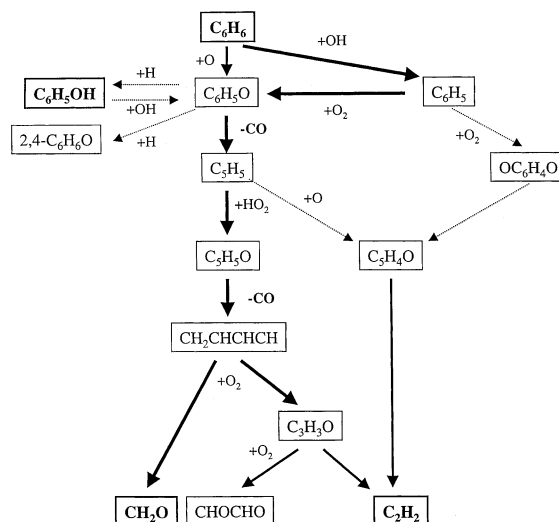
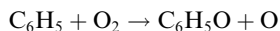


Fig. 9. Destruction-pathway diagram of  $C_6H_6$  at 993 K, using the mechanism of Marinov et al. Relative flux through pathways are proportional to the arrow width. Species in bold were experimentally measured.

In Fig. 8, the Zhang and McKinnon (1995) reaction-pathway diagram, the dominant destruction pathway for  $C_6H_6$  is through H abstraction by OH to form  $C_6H_5$ , with a secondary path through O substitution to directly form  $C_6H_5O$ . The  $C_6H_5$  reacts with molecular oxygen to form either  $C_6H_5O$  or  $C_2$  products. The  $C_6H_5O$  expels CO to form  $C_5H_5$ . The majority of the  $C_5H_5$  reacts with  $HO_2$  and follows a similar expulsion cycle (i.e., oxidation, and CO expulsion). The direct oxidation of  $C_6H_5$  to  $C_2$  products is described by a global reaction. The inclusion of a global reaction is unfortunate, but is required (to some degree) since details of benzene oxidation at these concentrations and temperatures are not complete. While Tan and Frank (1996) suggest that the use of this global reaction path is inappropriate, without the global reaction concentrations of  $C_2$  species (e.g., acetylene and ethylene) are significantly underpredicted. There is also a global reaction for the destruction of  $C_5H_4O$  directly to  $C_2$  products.

For the Marinov et al. (1996) reaction-pathway diagram (Fig. 9), the same general  $C_6$  chemistry is seen and nearly all of the reaction occurs through the  $C_6 \rightarrow C_5 \rightarrow C_4$ , CO-expulsion pathway. After  $C_6H_5$  and  $C_6H_5O$  are formed, the subsequent breakdown of the aromatic ring is dominated by different reactions than for the Zhang and McKinnon (1995) mechanism. In particular, progression from  $C_6$  to  $C_5$  is described with fundamental reactions. The  $C_5H_4O$  reactions are grouped into one global reaction producing  $C_2$  products, while reactions of  $C_5H_5O$  are modeled with fundamental reactions.

Both mechanisms have the same fundamental  $C_6$  chemistry, where breakdown of  $C_6H_6$  is predicted at low temperatures due to an efficient chain-branching pathway:



These reactions convert one radical (OH) into two ( $\text{C}_6\text{H}_5\text{O}$  and O). Standard  $\text{H}_2/\text{O}_2$  chemistry converts the O back into OH and the cycle repeats. Equilibrium concentrations of OH in the combustion-products flow efficiently initiate this reaction pathway at the low temperatures. Without this chain branching reaction, little destruction of  $\text{C}_6\text{H}_6$  is predicted. This is the primary reason the mechanism of Tan and Frank (1996) does not predict  $\text{C}_6\text{H}_6$  destruction at low temperatures.

The source of  $\text{CH}_2\text{O}$  in both mechanisms is the oxidation of products from the destruction of the aromatic ring. The lack of good agreement in  $\text{CH}_2\text{O}$  is probably not due to insufficient  $\text{C}_2$  chemistry, but rather a lack of fundamental chemistry describing the destruction of the aromatic ring. The Zhang and McKinnon (1995) mechanism used a global reaction step to produce  $\text{C}_2\text{H}_3$ , which then reacts with  $\text{O}_2$  to form  $\text{CH}_2\text{O}$ . The Marinov et al. (1996) mechanism formed  $\text{CH}_2\text{O}$  directly from the reaction of  $\text{C}_4\text{H}_5$  with  $\text{O}_2$ . Better prediction of the aromatic ring destruction to  $\text{C}_2$  species is needed to better understand the amounts of  $\text{CH}_2\text{O}$ ,  $\text{C}_2\text{H}_2$ , and  $\text{C}_2\text{H}_4$  seen in the experiments.

While there were some obvious differences in predicted peak concentrations and trends with temperature among the three mechanisms, the qualitative description of byproduct formation was generally good. There were three notable exceptions: (1) the lack of ethylene ( $\text{C}_2\text{H}_4$ ) prediction, (2) the lack of a viable phenol ( $\text{C}_6\text{H}_5\text{OH}$ ) oxidation pathway other than through phenoxy radicals ( $\text{C}_6\text{H}_5\text{O}$ ), and (3) incomplete fundamental  $\text{C}_5$  and  $\text{C}_4$  chemistry, as evidenced by  $\text{C}_1$  and  $\text{C}_2$  species predictions.

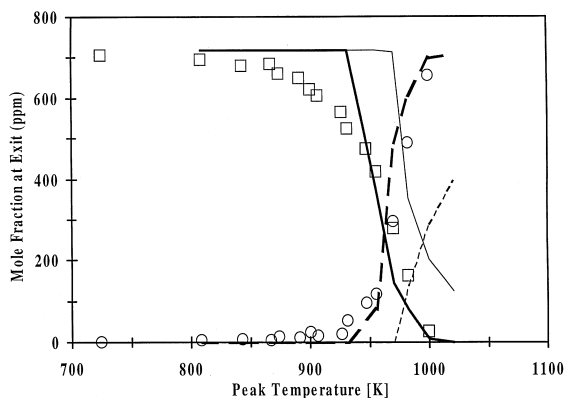


Fig. 10. Outlet concentration of  $\text{C}_6\text{H}_5\text{Cl}$  (squares) and HCl (circles) for the injection of  $\text{C}_6\text{H}_5\text{Cl}$ . Model data is plotted for  $\text{C}_6\text{H}_5\text{Cl}$  (solid lines) and HCl (dashed lines) using aggregate mechanisms based on the Zhang and McKinnon (thin lines) and Marinov et al. (thick lines) mechanisms.

## 7. Chlorobenzene oxidation

A similar analysis is used to investigate chlorobenzene ( $\text{C}_6\text{H}_5\text{Cl}$ ) oxidation. The experimental results for  $\text{C}_6\text{H}_5\text{Cl}$  oxidation (from 860 to 1000 K) cover conditions not used to validate any existing mechanisms. Measured byproducts include phenol ( $\text{C}_6\text{H}_5\text{OH}$ ), three isomers of chlorophenol (*o*-, *m*-, and *p*- $\text{C}_6\text{H}_4\text{ClOH}$ ), formaldehyde ( $\text{CH}_2\text{O}$ ), ethylene ( $\text{C}_2\text{H}_4$ ), vinyl chloride ( $\text{C}_2\text{H}_3\text{Cl}$ ), acetylene ( $\text{C}_2\text{H}_2$ ), and carbon monoxide (CO). The ultimate products of  $\text{C}_6\text{H}_5\text{Cl}$  (i.e.,  $\text{CO}_2$ , HCl, and  $\text{H}_2\text{O}$ ) were observed but only HCl was quantified. Molecular chlorine ( $\text{Cl}_2$ ) was not quantified since it is not detectable with an FTIR spectrometer. All of the experimental results for  $\text{C}_6\text{H}_5\text{Cl}$  oxidation are plotted in Figs. 10–15. The experimental data are plotted with the results from the modeling effort, using two aggregate chlorobenzene-oxidation mechanisms.

As seen in Fig. 4, the reactivity of chlorobenzene is similar to benzene. Examination of the experimental data reveals that the byproducts of chlorobenzene oxidation are similar in concentration and temperature range to benzene. For example, in Fig. 11 the peak concentration summed for all phenolic compounds is very close in magnitude and temperature as seen for benzene (Fig. 5). Similar byproduct trends for chlorobenzene and benzene are seen for  $\text{CH}_2\text{O}$ , CO, and  $\text{C}_2$  species.

The qualitative difference between benzene oxidation and chlorobenzene oxidation is found solely in the presence of chlorinated byproducts for chlorobenzene oxidation, which are analogous to the non-chlorinated byproducts measured for benzene oxidation. The lack of detectable  $\text{C}_4$  and  $\text{C}_5$  species is noted for both the benzene and chlorobenzene experiments.

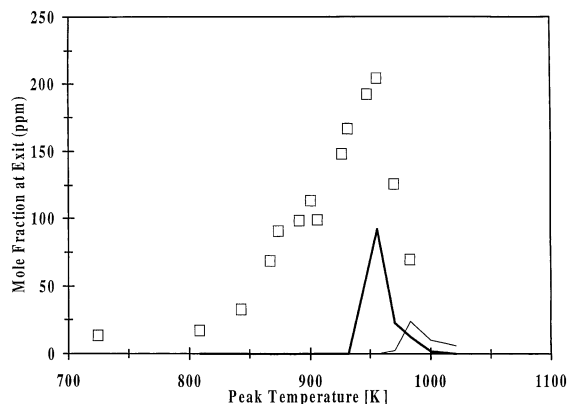


Fig. 11. Outlet concentration summed for all phenolic species,  $\text{C}_6\text{H}_5\text{OH}$ , *o*-, *m*-, and *p*- $\text{C}_6\text{H}_4\text{ClOH}$  (squares) for the injection of  $\text{C}_6\text{H}_5\text{Cl}$ . Modeled data is plotted as the sum of all phenol, chlorophenol, phenoxy and chlorophenoxy isomers using aggregate mechanisms based on the Zhang and McKinnon (thin line) and Marinov et al. (thick line) mechanisms.

Initial modeling efforts, using the mechanism of Martinez et al. (1995), predicted only 5% destruction of chlorobenzene at 1000 K. This mechanism also did not include chlorinated intermediate species. Most chemical-kinetic studies of chlorobenzene have focused on fuel rich and/or pyrolytic conditions. The resulting destruction pathways relied heavily on a C–Cl scission to initiate reaction. The bond dissociation energy for the C–Cl bond in chlorobenzene is about 15% less than the C–H bond in benzene. When pure or inert-diluted chlorobenzene is pyrolyzed, the weaker bond strength results in C–Cl scission as the dominant route of unimolecular chlorobenzene decomposition. Further, in a dilute atmosphere, chlorinated hydrocarbon byproducts are reduced, since the liberated chlorine radical quickly abstracts hydrogen to form HCl. The C–Cl scission step is weakly chain branching and does not provide for the oxidation of chlorobenzene observed at lower temperatures (e.g., 1000 K), which requires a stronger chain-branching mechanism to describe the measured results.

## 8. Chlorobenzene oxidation via benzene analogy

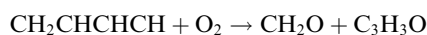
Based on the above observations, the chain-branching destruction pathway seen for benzene is proposed to exist for chlorobenzene oxidation as well. This is used to develop chemical-kinetic modeling that adequately describes the experimental results. Two chlorobenzene chemical-kinetic mechanisms are developed. One was developed based on the benzene mechanism of Zhang and McKinnon (1995) and the other based on Marinov et al. (1996). Two mechanisms were created because it is not the intent of this paper to develop a chemical-kinetic mechanism; rather it is to test the idea that benzene and chlorobenzene undergo analogous reactions under the conditions of this study.

We hypothesize that chlorobenzene, under post-flame oxidative conditions, reacts similarly to benzene. Specifically, (1) there should be an efficient chain-branching initiation step to promote reaction at low temperature, and (2) there should be a CO-expulsion pathway analogous to the benzene mechanisms (Emdee et al., 1992; Zhang and McKinnon, 1995; Marinov et al., 1996).

Two chlorobenzene-oxidation mechanisms were assembled following the CO expulsion steps seen for benzene: initial hydrogen abstraction, followed by oxygen addition, leading to CO expulsion (repeated twice). The number of carbons in the ring is reduced (i.e.,  $C_6 \rightarrow C_5 \rightarrow C_4$ ) until the ring is no longer resonantly stabilized and the resulting  $C_4$  ring breaks into linear species. The chlorobenzene mechanism is complicated by the lower symmetry in chlorobenzene. Hydrogen abstraction from benzene creates a phenyl radical regardless of which hydrogen was abstracted, while hydrogen abstraction from chlorobenzene creates one of

the three chlorophenyl radical isomers, *ortho*-, *meta*-, or *para*-chlorophenyl.

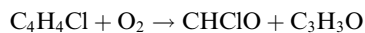
Reactions were sought to describe this destruction pathway. Using the NIST database (Mallard et al., 1998) and literature sources, 17 reactions describing chlorobenzene and chlorophenol reactions were found and included in each aggregate chlorobenzene mechanism. The reactions of chlorobenzene with OH, O and Cl were from Louw et al. (1973), Mulder and Louw (1987), Manion et al. (1988), Frerichs et al. (1989), Ritter et al. (1990), Qun and Senkan (1994) and Martinez et al. (1995). Unimolecular reactions of chlorobenzene were included from Ritter et al. (1990) and Martinez et al. (1995). Chlorophenol reactions were included from Mulder and Louw (1987). Destruction of the chlorophenyl radicals was assumed to follow the benzene analogy, and reaction rates from the benzene mechanisms were used to estimate the reaction rate of chlorophenyl radicals with molecular oxygen to create chlorophenoxy radicals. Further reactions include the addition of H to form chlorophenol, and the expulsion of CO to produce chlorinated  $C_5$  species. All of the chlorinated- $C_6$  reactions track the individual chlorinated isomers, and the rates of the reactions are approximated using the benzene reaction rates. Once  $C_5$  species are created, only one chlorinated isomer was assumed. Reactions were scaled to create chlorinated products in proportion to the number of possible isomers of the reactants. For example, consider



or similarly:



The analogous chlorinated reaction would have two outcomes:



and



Each outcome was given a pre-exponential reaction-rate factor equal to (2/5) and (3/5), respectively, to account for the relative quantities of chlorinated isomers. This procedure was repeated for every reaction in each parent benzene mechanism. Reactions with Cl substitution by H-atom attack have also been added for all chlorinated aromatic compounds. All reactions used are included in Tables 1, 2 and 3.

All of the original benzene chemistry is included in the aggregate mechanisms so that if the C–Cl bond is broken, the required chemistry is intact. Additionally, once chlorinated  $C_2$  species are reached, the added sub-mechanisms are capable of tracking the further evolution of these species.

In order for chemical-kinetic mechanisms to have broad utility, the specific reaction rates for each chlorinated reaction should be correctly derived and/or experimentally determined. Many of the reaction rates used in this analysis have been estimated using reaction rates from published benzene mechanisms. Care should be taken when using the rates in Tables 1, 2 and 3. The value of this work is to establish the direction required for the formulation of the reactions that are relevant to fuel-lean thermal oxidation of chlorobenzene.

## 9. Chlorobenzene oxidation results

The thermal oxidation of  $C_6H_5Cl$  between 860 and 1000 K produced measured quantities of  $C_6H_5OH$ , *o*-, *m*-, and *p*- $C_6H_4ClOH$ ,  $CH_2O$ ,  $C_2H_4$ ,  $C_2H_3Cl$ ,  $C_2H_2$ ,  $CO$ , and  $HCl$ . Experimental and numerical-modeling data, using aggregate mechanisms based on the benzene mechanisms of (1) Zhang and McKinnon (1995) and of (2) Marinov et al. (1996), are plotted in Figs. 10–15.

In Fig. 10, measured and predicted concentrations of the injected species,  $C_6H_5Cl$ , are plotted versus peak temperature. Overall, destruction of chlorobenzene is predicted well by the mechanism based on Marinov et al. (1996), although it slightly underpredicts chlorobenzene destruction below 950 K. The Zhang and McKinnon-based mechanism predicts chlorobenzene reaction only above 970 K. Also plotted in Fig. 11 are  $HCl$  concentrations. At the highest temperature (1000 K), most of the measured chlorine appears to have been converted to  $HCl$ . One-to-one conversion of  $Cl$  from  $C_6H_5Cl$  to  $HCl$  is difficult to determine since  $HCl$  was hard to measure accurately and  $Cl_2$  was not detectable with an FTIR spectrometer. At 1000 K, the Marinov-based mechanism

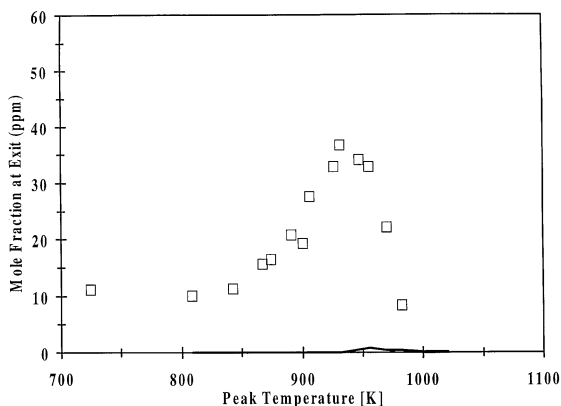


Fig. 12. Outlet concentration of  $C_6H_5OH$  (squares) for the injection of  $C_6H_5Cl$ . Modeled data plotted as the sum of  $C_6H_5OH$  and  $C_6H_5O$  using aggregate mechanisms based on the Zhang and McKinnon (thin line) and Marinov et al. (thick line) mechanisms.

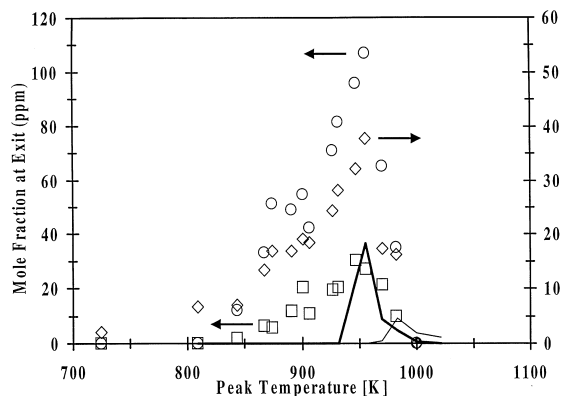


Fig. 13. Outlet concentration of *o*- $C_6H_4ClOH$  (squares, left axis), *m*- $C_6H_4ClOH$  (circles, left axis), and *p*- $C_6H_4ClOH$  (diamonds, right axis) for the injection of  $C_6H_5Cl$ . Modeled data plotted as the sum of  $C_6H_4ClOH$  and  $C_6H_4ClO$  for each isomer, using aggregate mechanisms based on the Zhang and McKinnon (thin line) and Marinov et al. (thick line) mechanisms.

predicted that only 0.4% chlorobenzene was converted to  $Cl_2$ , a maximum concentration of 3 ppm.

All of the phenolic compounds (*o*-, *m*-, *p*- $C_6H_4ClOH$  and  $C_6H_5OH$ ) were summed and plotted in Fig. 11. The numerical results also include the phenoxy and chlorophenoxy radicals, *o*-, *m*-, *p*- $C_6H_4ClO$  and  $C_6H_5O$ . The peak concentration of these species reached 205 ppm at 956 K. This equates to a yield of 71% of the reacted chlorobenzene and occurs when about 60% of the chlorobenzene were destroyed. These numbers are relatively close to those found for the benzene oxidation case. The Marinov-based mechanism accurately predicts the temperature at which the phenolic compounds peak, but the magnitude is underpredicted by a factor of two.

In Fig. 12, phenol ( $C_6H_5OH$ ) concentrations are plotted. Peak quantities of  $C_6H_5OH$  occur at 932 K with a maximum concentration of 36 ppm. This occurs about

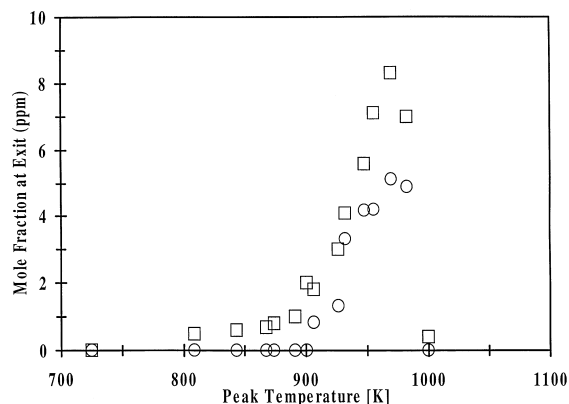


Fig. 14. Outlet concentration of  $C_2H_4$  (squares), and  $C_2H_3Cl$  (circles) for the injection of  $C_6H_5Cl$ . Neither mechanism predicted significant  $C_2H_4$  or  $C_2H_3Cl$  concentrations.

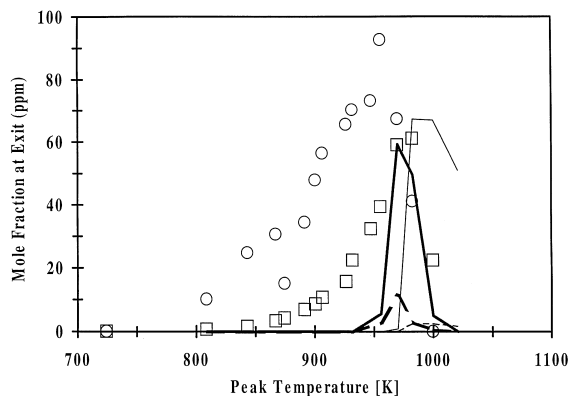


Fig. 15. Outlet concentration of  $C_2H_2$  (squares), and  $CH_2O$  (circles) for the injection of  $C_6H_5Cl$ . Modeled data plotted for  $C_2H_2$  (solid lines) and  $CH_2O$  (dashed lines) using aggregate mechanisms based on the Zhang and McKinnon (thin lines) and Marinov et al. (thick lines) mechanisms.

20 K lower, with approximately one-sixth the yield of the  $C_6H_6$  experiments. Both mechanisms poorly predicted  $C_6H_5OH$ , indicating that they still lack important Cl-abstraction or substitution reactions. It is doubtful that the  $C_6H_5OH$  is underpredicted due to poorly estimated reaction rates since all of the reactions leading to  $C_6H_5OH$  were taken directly from literature sources. The three isomers of chlorophenol are plotted individually in Fig. 13 and have maximum concentrations of 30, 107, and 38 ppm, respectively, occurring near 950 K (Note, there are two *meta*- and *ortho*-substitution sites, but only one *para*-substitution site). To ease comparison, the data for  $C_6H_5OH$  (Fig. 12) and *p*- $C_6H_4ClOH$  (Fig. 13, right axis) are plotted with an ordinate scale that is twice that of *o*- and *m*- $C_6H_4ClOH$  (Fig. 13, left axis). By doing this, the phenolic compounds are plotted in proportion to the number of substitution sites. It is easy to see that the experimental data for  $C_6H_5OH$ , *p*- $C_6H_4ClOH$ , and *m*- $C_6H_4ClOH$  all have approximately the same trends and the same peak quantities (per substitution site). Additionally, plotting the numerical data in this manner causes all to fall on top of one curve (for each mechanism). This happens because the reaction-rate data were scaled proportionally to the number of substitution sites.

The experimental data for *o*- $C_6H_4ClOH$  differs from the other phenolic compounds, with much lower concentrations. This can be explained by a combination of geometric and electrophilic effects: the adjacent Cl atom physically shields the hydrogen, and the electrophilic nature of the Cl atom shortens the H bond length making it stronger and less reactive. These effects have not been considered when estimating the chemical-kinetic rates; doing so should give results that are qualitatively closer to the measure data.

Four minor byproducts were observed at peak concentrations less than 100 ppm, including  $CH_2O$  at 93

ppm,  $C_2H_2$  at 61 ppm,  $C_2H_4$  at 8.3 ppm and  $C_2H_3Cl$  at 5.1 ppm. In Fig. 14, data for  $C_2H_3Cl$  and  $C_2H_4$  are plotted. In Fig. 15, data for  $C_2H_2$  and  $CH_2O$  are plotted.  $C_2H_3Cl$  was the only non-aromatic chlorinated hydrocarbon detected. The three  $C_2$  species peak at nearly the same temperature (980, 980, and 970 K), which is slightly higher than the peak  $C_6H_5OH$  and  $CH_2O$  temperature but less than that for peak of CO. Maximum concentrations for  $C_2H_2$  and  $C_2H_4$  occur at nearly identical peak temperatures as seen for  $C_6H_6$ .

Of the four minor byproducts, only  $C_2H_2$  and  $CH_2O$  were predicted by the two mechanisms.  $C_2H_3Cl$  and  $C_2H_4$  were not predicted at levels above 10 ppb. No significant concentrations of other stable chlorinated species were predicted by the mechanisms. The Marinov-based mechanism predicts  $C_2H_2$  well, but  $CH_2O$  was underpredicted and with a higher peak temperature. These results are likely to be due to the chlorinated  $C_5$ ,  $C_4$  and  $C_3$  chemistry. The poor prediction of  $C_2H_3Cl$  from chlorobenzene oxidation is analogous to the poor prediction of  $C_2H_4$  in benzene oxidation. Chlorinated  $C_5$  and  $C_4$  compounds are required to explain the production of vinyl chloride.

## 10. Chlorobenzene oxidation destruction pathway (1000 K)

Fig. 16 shows the principal reaction pathways of chlorobenzene using the Marinov-based chlorobenzene mechanism. The principal reaction pathways from the chlorobenzene mechanisms based on the work of Zhang and McKinnon (1995) are essentially identical. Only the significant  $C_6$  chemistry is included in the figure.  $C_5$ – $C_1$  species show the same dominant trends seen for each benzene mechanism used to develop the two aggregate chlorobenzene mechanisms.

The two main pathways for initial  $C_6H_5Cl$  destruction are through H abstraction by OH to form  $C_6H_4Cl$  and through O substitution to directly form  $C_6H_4ClO$ . The

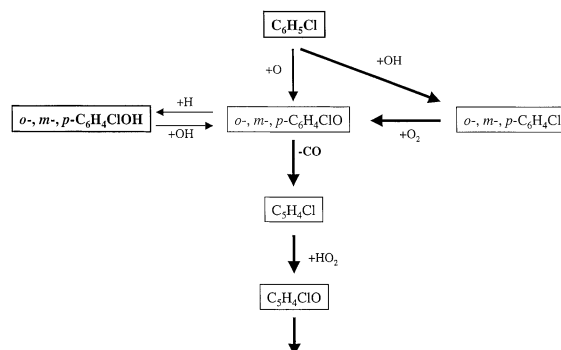
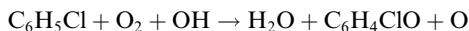
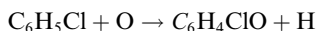


Fig. 16. Destruction-pathway diagram of  $C_6H_5Cl$  at 1000 K, using the aggregate chlorobenzene mechanism based on Marinov et al. Relative flux through pathways are proportional to the arrow width. Species in bold were experimentally measured.

$C_6H_4Cl$  undergoes molecular oxygen attack to form  $C_6H_4ClO$ . Passing through  $C_6H_4ClO$ , CO is expelled to form  $C_5H_4Cl$ , which follows a similar expulsion cycle (i.e., oxidation, and CO expulsion) leading to products. The  $C_6$  chemistry is the same as for benzene with the following distinctions. Destruction of  $C_6H_5Cl$  is initiated by the same chain branching seen for the benzene case. Grouping the  $C_6$  reactions gives two dominant pathways:



and



The first is chain branching and the second is chain propagating. It is these reactions and the equilibrium concentrations of OH in the combustion-products flow that result in efficient destruction of chlorobenzene at low temperatures. Note that most of the rates for the chain-branching,  $C_6$ -species reactions were taken from literature sources and were not estimated from benzene reaction rates. The majority of the estimated reaction rates were for reactions not containing  $C_6$  species.

Chlorophenol,  $C_6H_4ClOH$ , was also formed. Due to the relative stability of phenolic compounds, formation is chain terminating and slows the destruction of  $C_6H_5Cl$ . Similar to benzene, destruction of  $C_6H_4ClOH$  is only predicted to occur back through  $C_6H_4ClO$ . The bond dissociation energy of the phenolic hydrogen is still only about 90% that of the ring hydrogen and direct destruction or continued oxidation is probable, but not predicted.

No significant amount of dechlorination of the chloroaromatic compounds is predicted. This is responsible for the underprediction of phenol and indicates that Cl-removal reactions are missing from the mechanisms.

## 11. Summary of chlorobenzene oxidation

These results support the idea that the thermal oxidation pathways of chlorobenzene are analogous to those of benzene. As the reaction mechanism of benzene becomes better understood, it is expected to also improve the chlorobenzene mechanism. Until the  $C_5$  and  $C_4$  chemistry in the benzene mechanism is firmly established, chlorinated  $C_5$  and  $C_4$  chemical-kinetic destruction pathways will be difficult to determine accurately. Deficiencies in the chlorobenzene mechanisms presented here include the reaction rates for elementary chlorophenyl and chlorophenol oxidation reactions, detailed chlorinated- $C_5$  and - $C_4$  chemistry, and the formation pathways to directly produce chlorinated  $C_2$  species from chlorinated  $C_4$  species.

The absence of vinyl chloride ( $C_2H_3Cl$ ) and ethylene ( $C_2H_4$ ) prediction is analogous to the absence of  $C_2H_4$  prediction in the benzene case. There is sufficient sub-chemistry in the model to account for  $C_2H_3Cl$  if it were

to produce by the chlorination of combustion byproducts. This suggests that  $C_2H_3Cl$  is probably originating from chlorinated  $C_5$  and  $C_4$  species, just as  $C_2H_4$  is probably originating from  $C_5$  and  $C_4$  species in the benzene case.

## 12. Conclusions

The results of an experimental flow reactor study of the thermal oxidation of benzene and chlorobenzene have produced some interesting mechanistic conclusions. Although much work has been published on benzene chemical kinetics, most of it has focused on conditions different to those used in this study. The chemical-kinetic mechanisms of Emdee et al. (1992), Zhang and McKinnon (1995), and Marinov et al. (1996) did a suitable job of describing post-flame benzene destruction under thermal oxidation conditions. Most of the measured byproducts were predicted and the trends were usually adequate, however, the magnitude of the predictions was typically beyond the experimental error of the measurements. Although the chemical-kinetic mechanisms have evolved and improved considerably, trace byproduct prediction still requires more work before reliable results in real-life environments are realized.

Published chlorobenzene reaction mechanisms did a poor job of predicting oxidation of the parent species for the temperatures and species concentrations used in this study. This is not unexpected since most studies focused on pyrolytic conditions. Furthermore, literature sources of reaction rates did not cover all reactions occurring in this regime (e.g., chlorophenol destruction reactions) and reaction rates were estimated using the benzene mechanisms.

Experimentally, chlorobenzene was slightly less reactive than benzene. A destruction scheme was proposed, analogous to benzene oxidation, where chlorobenzene oxidation occurs through hydrogen abstraction followed by CO expulsion. Hydrogen-abstraction reactions, leading to efficient, low-temperature chain branching, were essential for predicting the destruction of chlorobenzene at 900 K. In addition, C–Cl scission reactions and Cl substitution reactions were not found to dominate at the temperatures and background species concentrations (combustion products) used in this study. The analysis was complicated by the reduced symmetry of chlorobenzene, which introduces many more chlorinated isomers.

Since the relative dissociation bond energies between phenolic and ring hydrogens are nearly the same, continued reaction of phenol and chlorophenol is also expected, resulting in destruction routes of the phenolic compounds that are different than the formation routes.

The lack of predicted  $C_2H_4$  from both benzene and chlorobenzene and  $C_2H_3Cl$  from the chlorobenzene

suggests (1) the more C<sub>5</sub> to C<sub>2</sub> chemistry is needed, and (2) that vinyl chloride is probably originating from chlorinated C<sub>5</sub> and C<sub>4</sub> species.

With the lack of an active C–Cl scission reaction pathway, chlorobenzene oxidation under moderate temperatures and oxygen-rich conditions leads primarily to chlorinated byproducts, where the stability of the aromatic ring structure could provide routes to significantly more toxic chlorinated byproducts.

## References

- Bittker, D.A., 1991. Detailed mechanism for oxidation of benzene. *Combust. Sci. Technol.* 79 (1–3), 49–72.
- Brezinsky, K., Lovell, A.B., Glassman, I., 1990. The oxidation of toluene perturbed by NO<sub>2</sub>. *Combustion Science and Technology* 70, 33–46.
- Chen, J.-Y., 1992. A perfectly-stirred-reaction description of chemistry in turbulent non-premixed combustion of methane in air. *Combust. Sci. Technol.* 84, 45–50.
- Dean, A.M., 1985. Predictions of pressure and temperature effects upon radical-addition and recombination reactions. *J. Phys. Chem.* 89, 4600–4608.
- Dean, A.M., Bozzelli, J.W., Ritter, E.R., 1991. CHEMACT: A computer code to estimate rate constants for chemically activated reactions. *Combust. Sci. Technol.* 80, 63–85.
- Emdee, J.L., Brezinsky, K., Glassman, I., 1992. A kinetic-model for the oxidation of toluene near 1200 K. *J. Phys. Chem.* 96 (5), 2151–2161.
- Frerichs, H., Tappe, M., Wagner, H.G., 1989. Reactions of fluorobenzene, chlorobenzene and bromobenzene with atomic oxygen (O<sup>3</sup>P) in the gas phase. *Z. Phys. Chem. Neue Folge* 162 (2), 147–159.
- Hall, M.J., Lucas, D., Koshland, C.P., 1991. Measuring chlorinated hydrocarbons in combustion by use of Fourier-Transform infrared spectroscopy. *Environmental Science and Technology* 25, 260–267.
- Higgins, B.S., 1995. Experimental development of a combustion-driven flow reactor to study post-flame, thermal oxidation of chlorinated hydrocarbons. Doctoral Dissertation. University of California, Berkeley, CA.
- Kee, R.J., Rupley, F.M., Miller, J.A., 1990. CHEMKIN II: A Fortran Chemical Kinetics Package for the Analysis of Gas-Phase Chemical Kinetics. Sandia National Laboratories, Livermore, CA.
- Louw, R., Rothuizen, J.W., Wegman, R.C.C., 1973. Vapour phase chemistry of arenes. Part II. Thermolysis of chlorobenzene and reactions with aryl radicals and chlorine and hydrogen atoms at 500 K. *J. Chem. Soc. Perkins Trans.* 2, 1635–1640.
- Lovell, A.B., Brezinsky, K., Glassman, I., 1988. Benzene oxidation perturbed by NO<sub>2</sub> addition. 22nd Symposium (International) on Combustion. The Combustion Institute, pp. 1063–1074.
- Oppelt, E.T., 1986. Hazardous-waste destruction. *Environ. Sci. Technol.* 20 (4), 312–318.
- Mallard, W.G., Westley, F., Herron, J.T., Hampson, R.F., Frizzell, D.H., 1998. NIST Chemical Kinetic Database, NIST, Washington, DC.
- Manion, J.A., Dijks, J.H.M., Mulder, P., Louw, R., 1988. Studies in gas-phase thermal hydrogenolysis. Part IV: chlorobenzene and *o*-dichlorobenzene. *Rec. Trav. Chim. Pays-Bas* 107 (6) 434–439 (*J. R. Netherlands Chem. Soc.*).
- Manion, J.A., Louw, R., 1990. Relative gas-phase desubstitution rates of chlorobenzene derivatives by hydrogen atoms near 1000 K. *J. Chem. Soc. Perkins Trans. II* (4), 551–557.
- Marinov, N.M., Pitz, W.J., Westbrook, C.K., Castaldi, M.J., Senkan, S.M., 1996. *Combust. Sci. Technol.* 116 (1–6), 211–287.
- Martinez, A., Cooper, C.D., Clausen, C.A., Geiger, C., 1995. Kinetic modeling of H<sub>2</sub>O<sub>2</sub> enhanced incineration of heptane and chlorobenzene. *Waste Manage.* 15 (1), 43–53.
- Mulder, P., Louw, R., 1987. Vapour-phase chemistry of arenes. Part 13. Reactivity and selectivity in the gas-phase reactions of hydroxyl radicals with monosubstituted benzenes at 563 K. *J. Chem. Soc. Perkins Trans.* 2 (9), 1167–1173.
- Qun, M., Senkan, S.M., 1994. Chemical kinetic modeling of fuel-rich flames of CH<sub>2</sub>Cl<sub>2</sub>/CH<sub>4</sub>/O<sub>2</sub>/Ar. *Combust. Sci. Technol.* 101, 103–134.
- Ritter, E.R., Bozzelli, J.W., 1990. Reactions of chlorinated benzenes in H<sub>2</sub> and in H<sub>2</sub>/O<sub>2</sub> mixtures: thermodynamic implications on pathways to dioxin. *Combust. Sci. Technol.* 74, 117–135.
- Ritter, E.R., Bozzelli, J.W., Dean, A.M., 1990. Kinetic study on thermal decomposition of chlorobenzene diluted in H<sub>2</sub>. *J. Phys. Chem.* 94 (6), 2493–2504.
- Ritter, E.R., Bozzelli, J.W., 1991. THERM: thermodynamic property estimation for gas-phase radicals and molecules. *Int. J. Chem. Kinet.* 23 (9), 767–778.
- Ritter, E.R., Bozzelli, J.W., 1994. Pathways to chlorinated dibenzodioxins and dibenzofurans from partial oxidation of chlorinated aromatics by OH radical: thermodynamic and kinetic insights. *Combust. Sci. Technol.* 101, 153–169.
- Roesler, J.F., Yetter, R.A., Dryer, F.L., 1995. Kinetic interactions of CO, NO<sub>x</sub>, and HCl emissions in postcombustion gases. *Combust. Flame* 100, 495–504.
- Senkan, S.M., 1993. Survey of rate constants in the C/H/Cl/O system. In: Gardiner, W.C. (Ed.), *Combustion Chemistry*, second ed. Springer, NY.
- Sommeling, P.M., Mulder, P., Louw, R., Avila, D.V., Luszyk, J., Ingold, K.U., 1993. Rate of reaction of phenyl radicals with oxygen in solution and in the gas phase. *J. Phys. Chem.* 97 (32), 8361–8364.
- Tan, Y., Frank, P., 1996. A detailed comprehensive kinetic model for benzene oxidation using the recent kinetic results. In: *Proceedings of the 26th Symposium (International) on Combustion*. The Combustion Institute, pp. 677–684.
- Tsang, W., 1990. Fundamental processes in the incineration of chloroaromatic compounds. *Air Waste Manage.* 10, 217–255.
- Venkat, C., Brezinsky, K., Glassman, I., 1982. High temperature oxidation of aromatic hydrocarbons. 19th Symposium (International) on Combustion, The Combustion Institute, pp. 143–152.
- Yang, M., Karra, S.B., Senkan, S.M., 1987. Equilibrium analysis of combustion incineration. *Hazard. Waste Hazard. Mater.* 4, 55–68.
- Zhang, H.-Y., McKinnon, J.T., 1995. Elementary reaction modeling of high-temperature benzene combustion. *Combust. Sci. Technol.* 107, 261–300.